JOURNAL OF SOLID STATE CHEMISTRY **44,** 282–289 (1982)

Hexagonal–Spinel Transitions in Antimonates $Li_2Cr_{3-x}M_x^{III}SbO_8$ (M^{III} = Al, Fe, Ga)

P. TARTE, R. CAHAY, J. PREUDHOMME

Université de Liège, Institut de Chimie, B-4000 Sart-Tilman par Liège 1, Belgium

AND M. HERVIEU, J. CHOISNET, AND B. RAVEAU

Laboratoire de Cristallographie et Chimie du Solide, L.A. 251, ISMRA–Université de Caen, 14032 Caen Cedex, France

Received February 22, 1982; in final form May 4, 1982

A new family of antimonates $Li_2Cr_{3-x}M_x^{III}SbO_8$ (M^{III} = Al, Fe, Ga) was synthesized and studied by X-ray diffraction and ir spectroscopy. The Al-containing compounds exhibit a hexagonal close-packed structure similar to that of $LiFeSnO_4$ ($a \simeq 5.8$, $c \simeq 9.5$ Å). For M = Fe or Ga, two structural forms are isolated: a low-temperature hexagonal form which is isotypic with $LiFeSnO_4$ and a high-temperature cubic form isotypic with the spinel structure. The hexagonal spinel transformation was observed for the first time, while the reverse transformation cannot be obtained.

Introduction

Many oxides corresponding to the formulation M_3O_4, where M can correspond to several ions of different nature, but with a small size ($R < 0.8$ Å), are characterized by a spinel structure. In this respect, the antimonates exhibit a particular behavior. A spinel structure has indeed been reported for $Li_2Cr_3SbO_8$ and $Li_2Rh_3SbO_8$ (*1*), but no spinel phase was found in the case of $Li_2Fe_3SbO_8$ (*1*). In the same way, although several stannates exhibit the spinel structure, two of them—$LiFeSnO_4$ (*2*) and $Li_{1.6}M_{1.6}Sn_{2.8}O_8$ (M = Mg, Zn) (*3*)—are characterized by a hexagonal close packing related to that of spinel. Thus the stability of the hexagonal structure could be due to the presence of an nd^{10} cation. In connection with the previous work by some of us (*4, 5*) on the order–disorder phenomena in antimonates with a spinel structure, we thus considered the antimony oxides $Li_2Cr_{3-x}M_x^{III}SbO_8$. The present paper deals with the fairly systematic investigation of the chemical and structural aspects of this family of antimonates in order to determine the relative stability of the hexagonal and spinel structures.

Experimental

Synthesis of the compounds. Two different synthesis procedures were used:

(i) A stoichiometric mixture of Li_2CO_3 and the appropriate oxides (Sb_2O_3 and M_2O_3) is well ground under petroleum ether and very progressively heated in covered platinum crucibles.

(ii) A stoichiometric mixture of Li_2CO_3, elemental Sb, and M_2O_3 (or the metal itself) is submitted to a chemical attack by nitric

0022-4596/82/110282-08$02.00/0

acid, followed by evaporation to dryness and thermal treatment. This leads to more homogeneous and more reactive systems.

Whatever the starting procedure may be, the resulting mixture is repeatedly ground and heated at increasing temperatures, the result of each step being checked by X-ray diffractometry and infrared spectroscopy. This step by step procedure is necessary since some phases are stable (or even metastable) only in a fairly narrow temperature range. A few compounds were submitted to a hydrothermal treatment.

Analysis. All phases were investigated at room temperature by X-ray diffraction (monochromatized Co$K\alpha$ or Cu$K\alpha$ radiation), by electron diffraction (JEOL 100CX), and also by infrared spectroscopy (2000- to 250-cm^{-1} region: Beckman 4250 spectrometer, KBr disks; 350- to 15-cm^{-1} region: Polytec Fir 30 interferometer, polythene disks).

The lithium amount in these samples was determined by atomic absorption with a Varian spectrometer.

Results and Discussion

Investigation of $Li_2Cr_{3-x}M^{III}_xSbO_8$ Systems

The experimental results are given in Table I and may be summarized as follows:

—Four new polymorphous phases—$Li_2Fe_3SbO_8$, $Li_2Cr_2GaSbO_8$, $Li_2Cr_2FeSbO_8$, $Li_2Fe_2CrSbO_8$—were isolated. They exhibit a low-temperature hexagonal form and a high-temperature spinel form.

—Some phases do not exhibit polymorphism and were obtained either with the spinel structure only—$Li_2Rh_3SbO_8$ (*1*), $Li_2Cr_3SbO_8$ (*1*), and $Li_2Cr_2RhSbO_8$—or with the hexagonal structure only—$Li_2Cr_{3-x}Al_xSbO_8$ with $0.5 \leq x \leq 2.5$.

—Other attempts with composition, $Li_2Al_3SbO_8$, $Li_2Ga_3SbO_8$, $Li_2Cr_2InSbO_8$, and $Li_2Cr_2ScSbO_8$, always led to mixtures.

Chemical and Thermal Stability

The ease and conditions of formation of the hexagonal phase strongly depend on the nature of the M^{III} cation. For $Li_2Cr_2M^{III}SbO_8$ (M^{III} = Ga or Fe), the hexagonal phase is easily obtained in a pure (Fe) or nearly pure (Ga) state by heating the mixture of oxides at 900–1000°C; the transformation into the pure spinel phase is obtained at 1250–1300°C.

For $Li_2CrFe_2SbO_8$ and $Li_2Fe_3SbO_8$, however, the same procedure leads to a mixture of phases containing $LiSbO_3$, a spinel, and a small to negligible quantity of hexagonal phase. This is the result of the lower thermal stability of these compositions, which are stable only near or even below 700°C. At this relatively low temperature, the synthesis reaction is very sluggish and there is little hope for reaching the equilibrium state of the system; in addition, the diffraction peaks are not sharp.

Many experiments were carried out to overcome these difficulties, and we finally adopted the following procedure: the solid residue resulting from a chemical attack by nitric acid, followed by evaporation to dryness, is well ground and preheated at 600°C. This leads to a reactive mixture which is pelletized and heated for a short time (15 min) at 950°C.

We obtain in this way a well-crystallized hexagonal phase, together with a small quantity of $LiSbO_3$ and a spinel phase. Heating at higher temperatures or for a longer time increases the amount of impurities, but does not change the unit cell parameters of the remaining hexagonal phases. Their chemical composition is thus expected to be the same (or nearly the same) as that of the starting mixture, namely, $Li_2Fe_3SbO_8$ and $Li_2CrFe_2SbO_8$.

Crystallographic Data

All the patterns of these compounds were indexed either in a hexagonal cell by iso-

TABLE I

(h)-$LiFeSnO_4$ AND SPINEL-TYPE ANTIMONATES: CONDITIONS OF PREPARATION

Composition	Synthesis method	T (°C)	Results
$Li_2Cr_3SbO_8$ (*1*)	Oxides (i) Nitrates (ii)	950–1100	Spinel
$Li_2Rh_3SbO_8$	Oxides (i) Nitrates (ii)	850–1000	Spinel + $LiSbO_3$
$Li_2Fe_3SbO_8$	Oxides (i)	1000–1200 1250–1300	Mixtures ($LiSbO_3$ + spinel) Spinel
	Nitrates (ii)	See text 1250	Hexagonal Spinel
$Li_2Cr_{3-x}Al_xSbO_8$ $0.5 \leq x \leq 2.5$	Oxides (i)	1000–1300	Hexagonal
$Li_2Cr_2FeSbO_8$	Oxides	900–1000 1100–1200 1250–1300	Pure hexagonal phase Mixture ($LiSbO_3$ + spinel) Spinel
$Li_2CrFe_2SbO_8$	Oxides (i)	900–950 1000–1200 1250–1300	Very impure hexagonal phase Mixture ($LiSbO_3$ + spinel) Spinel
	Nitrates (ii)	See text 1250–1300	Nearly pure hexagonal phase Spinel
$Li_2Cr_2GaSbO_8$	Oxides (i)	900–1000 1050–1200 1250	Nearly pure hexagonal phase Mixture ($LiSbO_3$ + spinel) Nearly pure spinel
$Li_2Cr_2RhSbO_8$	Oxides (i)	900–1100	Spinel

typism with $LiFeSnO_4$ low-temperature form, noted (h)-$LiFeSnO_4$ (*2*), or in a cubic cell for the spinel-type phases. Unit cell parameters are given in Table II.

The parameters of the hexagonal phases strongly depend on the trivalent cation sizes. So, for example (Fig. 1), the replacement of chromium by aluminum involves a

TABLE II

$Li_2Cr_{3-x}M_xSbO_8$: CRYSTALLOGRAPHIC DATA

	Unit cell parameters of:			
	LT hexagonal phases			HT spinel phases
Composition	a (± 0.002 Å)	c (± 0.005 Å)	c/a	a (± 0.004 Å)
$Li_2Cr_3SbO_8$	—	—	—	8.391
$Li_2Cr_2AlSbO_8$	5.796	9.466	1.633	—
$Li_2Cr_2GaSbO_8$	5.847	9.508	1.626	8.350
$Li_2Cr_2FeSbO_8$	5.867	9.542	1.626	8.398
$Li_2CrFe_2SbO_8$	5.895	9.587	1.626	8.408
$Li_2Cr_{0.5}Al_{2.5}SbO_8$	5.703	9.392	1.647	—
$Li_2Fe_3SbO_8$	5.923	9.641	1.628	8.425

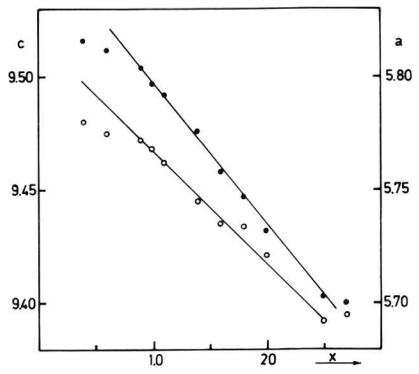

FIG. 1. Variation of a (solid circles) and c (open circles) parameters of hexagonal $Li_2Cr_{3-x}Al_xSbO_8$ with x.

significant decrease of a and c in a linear manner. On the other hand, the c/a ratio does not vary drastically but differs slightly from the ideal value.

Structural Study

Both structures, (h)-$LiFeSnO_4$ and spinel, can be described as a stacking along c of two sorts of polyhedral layers: octahedral layers (Oc) (Fig. 2a) and mixed layers (Te_2Oc) (Fig. 2b) formed of tetrahedra and octahedra. They differ by the stacking of the oxygen layers, which changes from |ABC–ABC| in the spinel to |ABAC| in the hexagonal structure, and by the types of cationic sites: the normal spinel structure contains only one type of tetrahedral and one type of octahedral site, whereas there are two types of tetrahedral and two types of octahedral sites in the (h)-$LiFeSnO_4$ structure. In order to determine the distributions in the different sites of these structures, six phases were studied from powder data: $Li_2Cr_2AlSbO_8$, $Li_2CrAl_2SbO_8$, and $Li_2Cr_2FeSbO_8$ high- and low-temperature forms, and $Li_2Fe_3SbO_8$ high- and low-temperature forms.

The intensities were registered on a Philips goniometer for Cu$K\alpha$ radiation. The space groups were studied on microcrystals by electron diffraction; for the hexagonal phases, the reflection conditions hhl, $l = 2n$, led to three possible space groups, $P\bar{6}2c$, $P6_3/mmc$, and $P6_3mc$, and for the cubic phases two groups were possible, Fd_3 and $Fd3m$.

Because of the analogy with (h)-Li $FeSnO_4$ and spinel compounds, respectively, the space groups $P6_3mc$ and $Fd3m$ were used for structural calculations.

(*a*) *Hexagonal phases.* The calculations were made, respectively, on the intensities of:

47 reflections for $Li_2Cr_2AlSbO_8$, i.e., 72 hkl,

42 reflections for $Li_2CrAl_2SbO_8$, i.e., 67 hkl,

45 reflections for $(Li_2Cr_2FeSbO_8)_{LT}$, i.e., 70 hkl,

66 reflections for $(Li_2Fe_3SbO_8)_{LT}$, i.e., 95 hkl.

The atoms were first distributed on the positions of the space group $P6_3mc$ previously used for $LiFeSnO_4$.

The atomic positions, the occupancy fac-

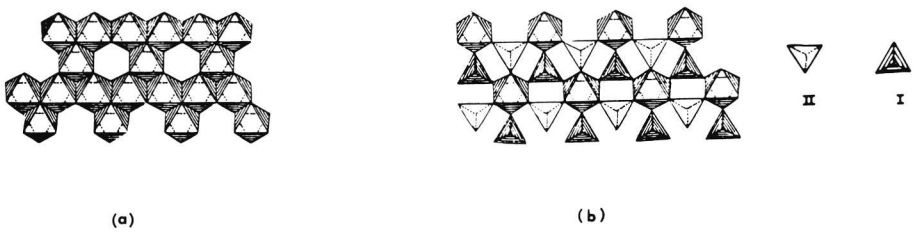

FIG. 2. Idealized drawing of hexagonal layers: (a) octahedral layer, (b) mixed layer.

tors of the metallic sites, and the thermal factors were successively refined, the occupancy sums being fixed to 1 for every cationic site. Good discrepancy factors, 0.039, 0.043, and 0.052, were thus obtained for $Li_2Cr_2AlSbO_8$, $Li_2CrAl_2SbO_8$, and $[Li_2Cr_2FeSbO_8]_{LT}$. For $[Li_2Fe_3SbO_8]_{LT}$, the discrepancy factor value could not be lowered under 0.09; it seems that several anomalous intensities are observed due to preferred orientation effects. Atomic parameters are close to those obtained for (h)-$LiFeSnO_4$ and $Li_{1.6}Sn_{2.8}Zn_{1.6}O_8$ (Table III). Table IV presents the distribution of metallic atoms on tetrahedral and octahedral sites.

Two distribution types are indicated: in $Li_2Cr_{3-x}M_xSbO_8$, the lithium ions are only located on the tetrahedral sites T_1 and T_2 and the antimony ions on the Oc_1 octahedral sites as tin in $(LiFeSnO_4)_{LT}$ and in $Sn_{2.8}Li_{1.6}Zn_{1.6}O_8$, while Cr and M ions are statistically distributed on Oc_2 octahedral sites: it is also worthy of note that aluminum is only located on octahedral sites.

In $Li_2Fe_3SbO_8$, an original distribution is observed. These results must be cautiously considered owing to the R value; nevertheless, the presence of antimony in $|Oc_1|$ and $|Oc_2|$ sites and the distribution of iron ions over the four types of sites appear as significant features.

Interatomic distances are close to those usually reported for tetrahedral and octahedral coordinations in hexagonal compact structures (Table V). They agree with the relative sizes of metallic ions: for example, in $Li_2CrAl_2SbO_8$, octahedral Oc_2 sites, where Al is located, show rather short distances compared to the other cases.

(*b*) *Infrared spectra of the hexagonal phases*. The ir spectra of the different hexagonal phases synthesized were recorded in

TABLE III

ATOMIC PARAMETERS OF HEXAGONAL PHASES: $Li_2Cr_{3-x}M_xSbO_8$ AND $Li_2Fe_3SbO_8$

	Sites		$Li_2Cr_2AlSbO_8$ $R = 0.039$	$Li_2CrAl_2SbO_8$ $R = 0.043$	$Li_2Cr_2FeSbO_8$ $R = 0.052$	$Li_2Fe_3SbO_8$ $R = 0.091$
T_1	(2*b*)	*z*	−0.116(10)	−0.076(14)	−0.097(6)	−0.072(2)
	$\frac{1}{3},\frac{2}{3},z$	*B* (Å²)	1	1	1	1.1
T_2	(2*a*)	*z*	0.512(16)	0.555(13)	0.523(12)	0.510(4)
	0,0,*z*	*B* (Å²)	1	1	1	1
Oc_2	(6*c*)	*x*	0.1724(8)	0.1660(4)	0.1710(4)	0.1697(2)
	$x,\bar{x},z$	*z*	0.2151(8)	0.2503(9)	0.2118(6)	0.204(1)
		B (Å²)	0.35	0.10	0.88	1.1
Oc_1	(2*b*)	*z*	0.4910(2)	0.5202(1)	0.4914(2)	0.4802(9)
	$\frac{1}{3},\frac{2}{3},z$	*B* (Å²)	0.15	0.38	0.57	1.2
O_1	(2*a*)	*z*	0.302(5)	0.338(3)	0.310(3)	0.304(4)
	0,0,*z*	*B* (Å²)	2.2	2.94	2.74	1.9
O_2	(2*b*)	*z*	0.090(4)	0.165(3)	0.101(4)	0.114(2)
	$\frac{1}{3},\frac{2}{3},z$	*B* (Å²)	1.2	1.27	0.10	1.8
O_3	(6*c*)	*x*	0.482(1)	0.490(1)	0.475(1)	0.481(1)
	$x,\bar{x},z$	*z*	0.346(4)	0.389(3)	0.365(4)	0.344(4)
		B (Å²)	1.95	2.12	2.73	1.8
O_4	(6*c*)	x	0.165(3)	0.171(1)	0.171(2)	0.180(4)
	$x,\bar{x},z$	*z*	0.596(4)	0.652(7)	0.598(5)	0.581(3)
		B (Å²)	0.70	0.85	1.23	2.9

TABLE IV

DISTRIBUTION OF THE METALLIC ATOMS IN THE HEXAGONAL ANTIMONATES

Compound	T_1	T_2	Oc_1	Oc_2
$Li_2Cr_2AlSbO_8$	Li	Li	Sb	Cr_2Al
$Li_2CrAl_2SbO_8$	Li	Li	Sb	$CrAl_2$
$Li_2Cr_2FeSbO_8$	Li	Li	Sb	Cr_2Fe
$Li_2Fe_3SbO_8$	$Li_{0.55}Fe_{0.45}$	$Li_{0.67}Fe_{0.33}$	$Sb_{0.67}Fe_{0.33}$	$Li_{0.78}Fe_{1.89}Sb_{0.33}$
(2) (h)-$Li_2Fe_2Sn_2O_8$	$Li_{0.56}Fe_{0.44}$	Li	Sn	$SnLi_{0.44}Fe_{1.56}$
(3) $Li_{1.6}Sn_{2.8}Zn_{1.6}O_8$	Zn	Li	Sn	$Sn_{1.8}Li_{0.6}Zn_{0.6}$

order to support the distribution of the metallic atoms, just described here. Two types of ir spectra were obtained, depending on the chemical composition.

(i) The ir spectrum of hexagonal $Li_2Cr_2FeSbO_8$ exhibits a series of sharp bands extending from 750 to about 200 cm^{-1} (Fig. 3), and very similar spectra are given by $Li_2Cr_2GaSbO_8$, $Li_2Cr_2AlSbO_8$, and the whole series $Li_2Cr_{3-x}Al_xSbO_8$. This sharpness is in agreement with the presence of one type of cation only (namely, Sb^V, M^{III}, and Li^I) on a given site. A detailed assignment of the bands is impossible. We can consider that the highest-valency cation (Sb^V) brings a major contribution to the highest-frequency bands (750–600 cm^{-1}); but it is very probable that no really localized vibration may exist in such a tridimensional structure. This is supported by the study of the ^6Li–^7Li isotopic shifts (Table

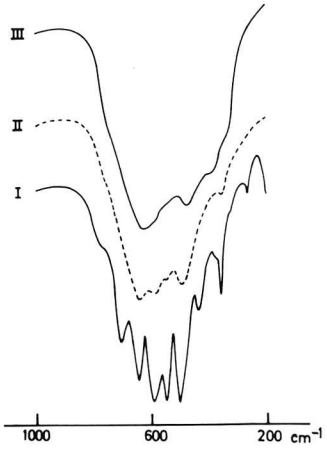

FIG. 3. Infrared spectra of hexagonal phases. I: $Li_2Cr_2FeSbO_8$; II: $Li_2CrFe_2SbO_8$; III: $Li_2Fe_3SbO_8$. The cation distribution is ordered in I, disordered in II and III.

TABLE V

INTERATOMIC DISTANCES IN HEXAGONAL ANTIMONATES (Å)

Polyhedron	$Li_2Cr_2AlSbO_8$		$Li_2CrAl_2SbO_8$	
T_1	T_1-O_2 (× 1)	1.95	T_1-O_2 (× 1)	2.26
	T_1-O_3 (× 3)	1.89	T_1-O_3 (× 3)	1.78
	O_2-O_3 (× 3)	2.97	O_2-O_3 (× 3)	3.12
	O_3-O_3 (× 3)	3.22	O_3-O_3 (× 3)	3.03
T_2	T_2-O_1 (× 1)	2.00	T_2-O_1 (× 1)	2.04
	T_2-O_4 (× 3)	1.84	T_2-O_4 (× 4)	1.93
	O_1-O_4 (× 3)	3.24	O_1-O_4 (× 3)	3.40
	O_4-O_4 (× 3)	2.87	O_4-O_4 (× 3)	2.94
Oc_2	Oc_2-O_1 (× 1)	1.92	Oc_2-O_1 (× 1)	1.87
	Oc_2-O_2 (× 1)	2.00	Oc_2-O_2 (× 1)	1.82
	Oc_2-O_3 (× 2)	1.99	Oc_2-O_3 (× 2)	2.06
	Oc_2-O_4 (× 2)	2.04	Oc_2-O_4 (× 2)	1.92
	O_1-O_3 (× 2)	2.93	O_1-O_3 (× 2)	2.91
	O_1-O_4 (× 2)	2.56	O_1-O_4 (× 2)	2.44
	O_2-O_3 (× 2)	2.84	O_2-O_3 (× 2)	2.62
	O_2-O_4 (× 2)	2.90	O_2-O_4 (× 2)	2.87
	O_3-O_3 (× 1)	2.58	O_3-O_3 (× 1)	2.70
	O_3-O_4 (× 2)	2.96	O_3-O_4 (× 2)	2.79
	O_4-O_4 (× 1)	2.87	O_4-O_4 (× 1)	2.94
Oc_1	Oc_1-O_3 (× 3)	2.02	Oc_1-O_3 (× 3)	1.99
	Oc_1-O_4 (× 3)	1.96	Oc_1-O_4 (× 3)	2.03
	O_3-O_3 (× 3)	2.58	O_3-O_3 (× 3)	2.70
	O_3-O_4 (× 6)	2.86	O_3-O_4 (× 6)	2.94
	O_4-O_4 (× 3)	2.92	O_4-O_4 (× 3)	2.79

TABLE VI

$^6Li-^7Li$ Isotopic Shifts in the ir Spectra of $Li_2Cr_2M^{III}SbO_8$ Phases

$Li_2Cr_2AlSbO_8$		$Li_2Cr_2GaSbO_8$		$Li_2Cr_2FeSbO_8$	
^6Li	^7Li	^6Li	^7Li	^6Li	^7Li
207	207	164	165	—	—
~297	~296	277	274	271	267
~312	~311	—	—	—	—
385	378	379	370	368	364
424	405	~410	~390	~405	~380
459	455	455	449	445	440

Note. Higher-frequency bands are not shifted by $^6Li-^7Li$ replacement.

VI); one band only, near 400 cm^{-1}, exhibits an isotopic shift of about 20 cm^{-1}, which is approximately the right order of magnitude for a Li translation in a LiO_4 tetrahedron (*6*). The smaller shifts observed for the remaining bands of the 450- to 250-cm^{-1} region suggest that these bands are related to mixed vibrations.

(ii) On the contrary, the ir spectrum of hexagonal $Li_2Fe_3SbO_8$ exhibits a small number of broad bands, whereas hexagonal $Li_2CrFe_2SbO_8$ appears to be an intermediate case (Fig. 3). This type of infrared pattern shows that the cation distribution is more or less disordered, and that the presence of Li and Fe on both tetrahedral and octahedral sites, already deduced from X-ray data for $Li_2Fe_3SbO_8$ (Table IV), is also true for $Li_2CrFe_2SbO_8$.

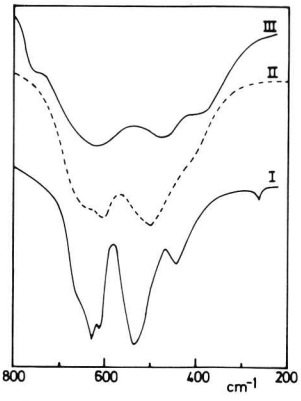

FIG. 4. Infrared spectra of spinel phases (I: $Li_2Cr_3SbO_8$; II: $Li_2Cr_2FeSbO_8$; III: $Li_2Fe_3SbO_8$) showing the influence of increasing disorder when going from I to III.

(*c*) *Spinel-type phases.* The intensity calculations were made for the high-temperature forms of $Li_2Cr_2FeSbO_8$ and $Li_2Fe_3SbO_8$ with 21 reflections (26 *hkl*) and 27 reflections (33 *hkl*), respectively. The atomic positions used are 8(*a*) tetrahedral sites, 16(*d*) octahedral sites, and 32(*e*) oxygen atoms of $Fd3m$ space group. The best values obtained for the *R* factors are obtained for the *x* parameter of oxygen and the thermal factors indicated in Table VII. The distribution of metallic ions on tetrahedral and octahedral sites are

$Li_2Cr_2FeSbO_8$: $[Li_{1.66}Fe_{0.34}]_T$ and $[Cr_2Fe_{0.66}Li_{0.34}Sb]_{Oc}$,

$Li_2Fe_3SbO_8$: $[Li_{0.88}Fe_{1.12}]_T$ and $[Li_{1.12}Fe_{2.88}Sb]_{Oc}$.

So, $[Li_2Fe_3SbO_8]_{HT}$ shows a strongly disordered distribution of metallic ions, as observed for $[Li_2Fe_3SbO_8]_{LT}$ hexagonal phase. The increase of the amount of disorder in these spinel phases, with the progressive replacement of Cr by Fe, clearly appears in the evolution of ir spectra in the significant broadening of the absorption bands (Fig. 4).

The Hexagonal–Spinel Transformation

Except for Al-containing compounds, for which the hexagonal phase is stable up to 1300°C, all the hexagonal antimonates, namely, $Li_2Cr_2FeSbO_8$, $Li_2Cr_2GaSbO_8$,

TABLE VII

Atomic Parameters of Spinel-Type Phases, $Fd3m$ S.G.

	8(*a*)	16(*d*)	32(*e*)	*R*
$[Li_2Cr_2FeSbO_8]_{HT}$	B = 1.5 Å^2	B = 0.6 Å^2	x = 0.384(1) B = 1.40 Å^2	0.066
$[Li_2Fe_3SbO_8]_{HT}$	B = 0.3 Å^2	B = 0.5 Å^2	x = 0.382(1) B = 0.7 Å^2	0.058

$Li_2CrFe_2SbO_8$, and $Li_2Fe_3SbO_8$, are transformed into the corresponding spinels by heating at a temperature close to 1250–1300°C.

However, this transformation does not seem to be direct. During the progressive heating of the hexagonal phase a mixture containing $LiSbO_3$ and a spinel whose unit cell parameter is generally different from that of the final $Li_2M_3SbO_8$ spinel always appear. A further increase of temperature brings out a progressive increase of the quantity of spinel phase, at the expense of $LiSbO_3$ which eventually disappears totally (or nearly so) at sufficiently high temperatures (1250–1300°C, depending on the chemical composition). The reverse (spinel to hexagonal) transformation has never been observed so far.

After tempering for 3 weeks at 1000°C, all iron-containing spinels exhibit extensive decomposition into $LiSbO_3$, and at least two cubic phases (most probably spinels) whose crystallinity (deduced from the sharpness of the diffraction peaks), unit cell dimensions, and relative quantities depend on the time of tempering. Even at this fairly high temperature, the evolution of the system is slow and it is highly probable that the equilibrium is not reached after 3 weeks. This instability at moderately high temperatures is in agreement with the lack of direct hexagonal–spinel transformation, and with the fact that Blasse was unable to synthesize $Li_2Fe_3SbO_8$ and 1150°C (*1*).

Hydrothermal experiments were also unsuccessful. $Li_2Cr_3SbO_8$ (spinel) remains unmodified after 1 week at 500°C and 1.5 kbar. After 1 week at 600°C and 1 kbar, hexagonal $Li_2Fe_3SbO_8$ is completely decomposed into a mixture containing well-crystallized $LiFeO_2$ and a spinel phase characterized by $a_0 = 8.344$ Å and $I_{111}/I_{220} = 0.1$; its ir spectrum is very similar to that of disordered $LiFe_5O_8$ (*7*). The formation of pure $LiFe_5O_8$ must be ruled out, since its unit cell parameter (8.332 Å) is smaller than the value obtained here. But Blasse has evidenced the formation of solid solutions of $Li_{1+x}Fe_{5-2x}Sb_xO_8$ for x up to 0.5 (*1*). The solid solution corresponding to $x = 0.2$ is characterized by a unit cell parameter of 8.345 Å and a disordered distribution of the cations. It is thus reasonable to consider that the spinel obtained by hydrothermal treatment of $Li_2Fe_3SbO_8$ is a solid solution similar to that described by Blasse, with x not very different from 0.2.

Conclusions

The systematic study of the antimonates $Li_2Cr_{3-x}M_x^{III}SbO_8$ showed the ability of these compounds to present either a hexagonal compact (h)-$LiFeSnO_4$-type structure or a spinel structure. The hexagonal–spinel transformation was observed for the first time. The iron compounds exhibit a particular behavior, especially in both forms of $Li_2Fe_3SbO_8$ for which a disordered distribution of iron is observed. These types of distributions should greatly influence the magnetic properties of these oxides, which will be investigated.

Acknowledgments

The authors (P.T., R.C., J.P.) gratefully acknowledge the financial support given to their laboratory by the "Fonds National de la Recherche Scientifique."

References

1. G. Blasse, *Philips Res. Rep.* **3**, 129 (1964).
2. J. Choisnet, M. Hervieu, B. Raveau, and P. Tarte, *J. Solid State Chem.* **40**, 344 (1981).
3. J. Choisnet and B. Raveau, *Mater. Res. Bull.* **14**, 1381 (1979).
4. P. Tarte and J. Preudhomme, *J. Solid State Chem.* **29**, 273 (1979).
5. J. Preudhomme, P. Tarte, R. Kenens, F. Grandjean, and A. Gerard, *Acad. Roy. Belg. Bull. Cl. Sci.* **66** [5], 776 (1980).
6. P. Tarte, *Spectrochim. Acta* **21**, 313 (1965).
7. P. Tarte and R. Collongues, *Ann. Chim.* **9** [13], 135 (1964).